JOURNAL OF SOLID STATE CHEMISTRY 45, 80–87 (1982)

Structure and Luminescence of the Orthorhombic $LnWO_4Cl$-Type Rare Earth Halo Tungstates*

L. H. BRIXNER, H. Y. CHEN, AND C. M. FORIS

E. I. du Pont de Nemours & Company Inc., Central Research and Development Department,† Experimental Station, Wilmington, Delaware 19898

Received April 29, 1982

$LaWO_4Cl$ is representative of a series of $LnWO_4Cl$ compounds in which *Ln* can be La to Sm. $LaWO_4Cl$ crystallizes in orthorhombic *Pbcm* symmetry, and its structure was refined using a disordered model to an *R* value of 4.0%. The most unusual structural feature is the 5-coordination of the W atom in the form of a trigonal bipyramid. The La atom is 9-coordinated. Luminescing ions, such as Sm, Tb, and Eu, were introduced into $LaWO_4Cl$ as a host, and their excitation and emission spectra are reported. The Raman spectrum of $LaWO_4Cl$ is compared to those of compounds containing W in more common tetrahedral and octahedral environments. X-Ray powder diffraction data are also reported.

Introduction

The composition $LaWO_4Cl$ was first described by Kharchenko *et al.* (*1*), who prepared it by a hydrothermal technique from $LaCl_3$ and WO_3. They described $LaWO_4Cl$ as crystallizing in orthorhombic symmetry, space group $Pbc2_1$. Kharchenko *et al.* (*1*) also indicated that $NdWO_4Cl$ and $CeWO_4Cl$ crystallize in the same structure. No detailed structural information is reported for these halo tungstates.

Since $LaWO_4Cl$ combines two heavy elements, the X-ray absorption of which falls within the medically useful energy range of 30 to 80 keV, it constituted an attractive host for doping with active rare earth ions. Since no fluorescing compounds based on $LaWO_4Cl$ are reported in the literature, the primary objective of this study was to prepare such materials and to determine the structure of $LaWO_4Cl$ in detail.

Experimental

A. Preparation

$LaWO_4Cl$, as well as all other $LnWO_4Cl$ compounds, was prepared by the interaction of *Ln*OCl with WO_3 in a sealed tube. For $LaWO_4Cl$, La_2O_3 (99.99% purity, Research Chemical Corp.) was dissolved in HCl, taken to dryness, and fired in air at 900°C to yield pure LaOCl. This component was then ball-milled with the stoichiometric amount of WO_3 (analytical grade, Fisher) and sealed into a quartz tube (1 cm diameter, 20 cm long). The reaction was carried out at 900°C for 8 to 10 hr and yielded pure $LaWO_4Cl$, with none of the constituent

* Presented at the Symposium on the Electronic Structure and Bonding in Solids, 183rd National Meeting, American Chemical Society, held in Las Vegas, Nevada, March 30–31, 1982.

† Contribution No. 3050.

0022-4596/82/130080-08$02.00/0

TABLE I

POSITIONAL AND THERMAL PARAMETERS FOR THE SUBCELL

Atom	x	y	z	B
W	0.25	0.6892(3)	0.32162(5)	0.15(2)
La	0.25	0.7460(3)	0.10374(8)	0.50(3)
Cl	0.25	0.248(2)	0.9877(3)	0.6(1)
O(1)	0.25	0.752(5)	0.2330(10)	0.8(4)
O(2)	0.25	0.238(5)	0.3237(9)	0.2(4)
O(3)	0.493(7)	0.750(4)	0.3692(10)	2.9(4)

components evident by X-ray examination. In order to obtain single crystals, about 50% LiCl was added to preformed La WO_4Cl. This mixture was sealed into a Pt tube, heated to 1100°C, and slow cooled at a rate of 5°C per hour. After leaching the excess flux with water, clear, colorless, single-crystalline plates of $LaWO_4Cl$ were obtained.

B. X-Ray Studies

1. Powder examination. The X-ray powder diffraction patterns of all $LnWO_4Cl$ preparations were obtained with a Guinier–Hägg-type focusing camera (radius 40 mm). The radiation was monochromatic Cu$K\alpha_1$ (λ = 1.5405 Å), and Si (a = 5.4305 Å) was used as an internal standard. Line positions on the film were determined to ±5 μm with a David Mann film reader (a precision screw, split-image comparator). Intensities were estimated by oscilloscopic comparison of film density with the strongest line of the pattern. Refined cell dimensions were obtained by a least-squares procedure (local program).

2. Single-crystal work. a. Data collection: A long, thin, plate-like crystal, about 0.2 × 0.066 × 0.033 mm, was mounted with the b axis nearly parallel to the spindle. Intensity data were collected at room temperature using a Syntex P3 diffractometer (graphite monochrometer, Mo$K\alpha$ radiation, λ = 0.71069 Å). From settings of 25 reflections, the lattice parameters of the orthorhombic cell were refined to a = 5.893(3), b = 7.856(4), and c = 19.270(9) Å. The systematic extinctions showed the presence of a b-glide with $0kl$: $k = 2n$, and a c-glide with $h0l$: $l = 2n$. In the ($hk0$) zone,

TABLE II

POSITIONAL AND THERMAL PARAMETERS FOR $LaWO_4Cl$ FULL-CELL STRUCTURE

	Atom	Mult.	x	y	z	B
1	W(1)	1.00	0.0008(3)	0.4714(1)	0.3201	0.33(1)
2	W(2)	0.92	0.4989(3)	0.2159(1)	0.1769(0)	0.11(1)
3	W(2A)	0.08	0.5053(3)	0.2559(1)	0.1776(5)	0.25(15)
4	La(1)	0.70	−0.0437(4)	0.4988(2)	0.0998(1)	0.38(3)
5	La(1A)	0.30	0.0582(8)	0.4980(5)	0.1080(2)	0.11(7)
6	La(2)	0.70	0.4482(3)	0.2520(2)	0.8930(1)	0.05(3)
7	La(2A)	0.30	0.5634(8)	0.2545(6)	0.8991(2)	0.39(8)
8	Cl(1)	1.00	0.0053(20)	0.2516(7)	0.4863(3)	1.20(8)
9	Cl(2)	1.00	0.5131(17)	−0.0000(6)	0.0104(2)	0.70(8)
10	O(1)	1.00	0.0072(46)	−0.0038(16)	0.2321(6)	0.16(21)
11	O(2)	1.00	0.5006(48)	0.2561(19)	0.2697(8)	0.93(25)
12	O(3)	1.00	0.7684(36)	0.2274(26)	0.1289(11)	1.66(37)
13	O(4)	1.00	0.2385(34)	0.2745(23)	0.1303(10)	1.15(32)
14	O(5)	1.00	0.2610(31)	0.5267(20)	0.3625(8)	0.38(26)
15	O(6)	1.00	0.2668(30)	−0.0307(19)	0.3633(8)	0.15(25)
16	O(7)	1.00	0.4300(27)	−0.0037(18)	0.1702(7)	0.22(25)
17	O(8)	1.00	0.0264(50)	0.2387(28)	0.3238(11)	2.97(44)

TABLE III

X-RAY POWDER DIFFRACTION DATA FOR $LaWO_4Cl$

2-θ	I/I_1	hkl	d_{obs}	d_{calc}
9.185	40	002	9.6201	9.6436
17.624	5	102	5.0279	5.0320
18.396	50	004	4.8187	4.8218
18.810	5	110	4.7134	4.7185
20.951	5	112	4.2365	4.2383
23.813	85	104	3.7333	3.7332
27.238	100	120	3.2712	3.2713
27.635	25	121	3.2252	3.2253
27.706	20	006	3.2170	3.2145
28.793	60	122	3.0980	3.0979
29.286	70	024	3.0469	3.0469
30.277	75	200	2.9494	2.9494
31.668	50	106	2.8230	2.8226
		202		2.8204
32.387	2	210	2.7620	2.7615
		025		2.7534
33.059	65	124	2.7073	2.7071
33.724	2	212	2.6554	2.6547
		116		2.6566
35.649	5	204	2.5163	2.5160
36.053	10	026	2.4890	2.4885
		125		2.4949
37.480	5	214	2.3975	2.3963
		130		2.3951
39.298	5	222	2.2907	2.2916
		126		2.2928
40.378	45	108	2.2318	2.2317
40.711	5	223	2.2144	2.2148
41.516	10	206	2.1732	2.1732
42.622	60	224	2.1194	2.1192
44.022	20	028	2.0552	2.0552
46.148	40	040	1.9653	1.9656
		300		1.9662
46.395	10	041	1.9554	1.9555
		230		1.9591
		119		1.9512
46.767	10	128	1.9408	1.9408
47.079	10	0010	1.9286	1.9287
		302		1.9266
		042		1.9260
47.630	10	310	1.9076	1.9075
47.784	35	226	1.9018	1.9020
		311		1.8982

Note. Plus 40 lines to $2\theta = 76°$.

there were many clear, though relatively weak, violations of the presence of the *a*-glide; thus the possible space group was *Pbcm* (No. 57) or $Pbc2_1$ (No. 29). Data were collected by the ω-scan technique with variable scan rates of 4 to 8° per minute over a 1.2° range. The scan time was equal to the background time. Empirical absorption corrections were carried out with ψ-scan data of three reflections, where the maximum variance of intensity was about 7%. 2029 reflections were collected in the quarter sphere of $(h,k,\pm l)$ with $2\theta \leqq 55°$.

The diffraction pattern showed a very strong subcell along the *b* axis. The averaged *E* values for $k = 2n + 1$ were about 0.05, compared to 1.87 for $k = 2n$. For the subcell, with $b' = b/2$, the systematic absences indicated the presence of an *n*-glide, $hk0$: $h + k = 2n$, in addition to the original *c*-glide. Thus the symmetry of the substructure approximated that of the space group *Pmcn* (No. 62).

b. Structure determination and refinement: All calculations were carried out on a PDP-11 computer, using local modifications of the structure determination package, SDP, supplied by the Enraf–Nonius Corp. (*2*). The atomic scattering factors were taken from the tabulations by Cromer and Waber (*3*). Anomalous dispersion corrections were by Cromer (*4*). In the full-matrix, least-squares refinement, the function minimized was $\Sigma w(|F_o| - |F_c|)^2$, for which

TABLE IV

INTERATOMIC DISTANCES (Å) AND BOND ANGLES (°) OF THE SUBCELL

W–O(1) × 1	1.727(9)	O(1)–W–O(2)	99.5(4)
W–O(3) × 2	1.717(15)	O(1)–W–O(2)	82.9(4)
W–O(2) × 1	1.773(8)	O(1)–W–O(3)	120.6(4)
W–O(2) × 1	2.157(8)	O(2)–W–O(2)	177.7(5)
		O(2)–W–O(3)	97.4(3)
		O(2)–W–O(3)	81.4(3)
		O(3)–W–O(3)	112.9(8)
La–O(1) × 1	2.492(9)		
La–O(3) × 2	2.523(12)		
La–O(3) × 2	2.549(12)		
La–Cl × 1	2.972(3)		
La–Cl × 1	2.983(3)		
La–Cl × 2	3.434(1)		

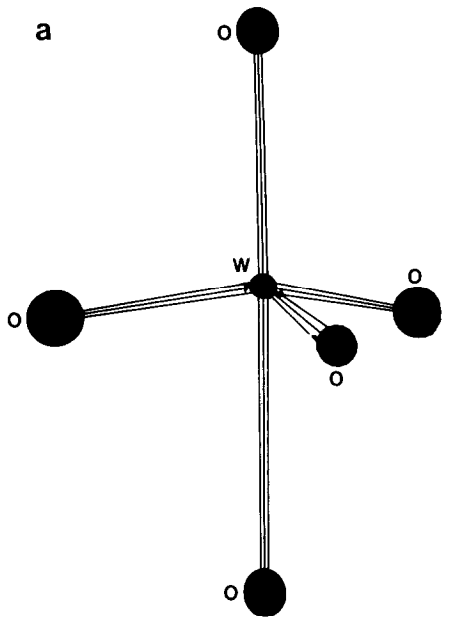

FIG. 1a. W coordination in $LaWO_4Cl$.

the weight, w, was the reciprocal of the value $\sigma(F^2) + 0.02F^2$.

The structure of the subcell was solved by the direct method for the heavy atoms, and by Fourier techniques for Cl and O. Subsequent refinements with 470 reflections converged to $R = 0.053$ and $R_w = 0.080$ with isotropic thermal parameters for all atoms. The results are shown in Table I.

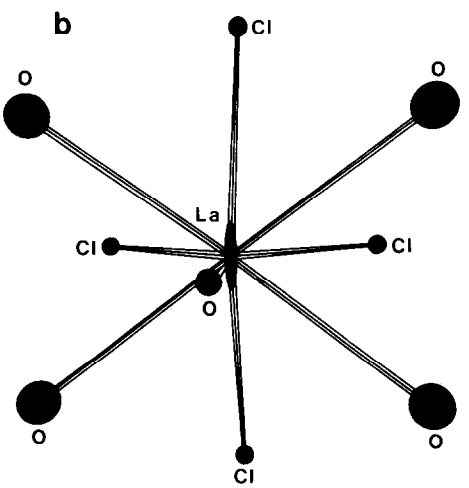

FIG. 1b. La coordination in $LaWO_4Cl$.

The R factors could be further reduced if the thermal parameters of W and La were refined anisotropically, but the refinements were not deemed meaningful, particularly with negative thermal parameters for the heavy atoms.

The subcell was then doubled along the b axis as an approximation to the full structure. It was found that the expanded structure was consistent with the accentric space group $Pbc2_1$ with the origin translated to $(\frac{1}{4}, -\frac{1}{8}, 0)$ with respect to the expanded cell. The refinement converged to $R = 0.059$ with isotropic thermal parameters for all atoms. A conversion to anisotropic thermal parameters for W and La atoms again led to nonpositive values for W and unusually large values for La atoms in the x direction. Moreover, the Fourier maps showed peaks split by a few tenths of an angstrom for these positions. Refinement in other space groups, including the monoclinic $P2_1/c$, did not eliminate the peak splitting. Finally, when the W and the La atoms were distributed evenly between the two split sites, the R factors improved significantly. The final values were 0.040 and 0.043, respectively, for R and R_w, with isotropic thermal parameters for all atoms and with the heavy atoms distributed between two sites within 0.5 Å of each other. The error in observation of the unit weight was $2.3e/Å$. Table II lists the positional and thermal parameters of all atoms in the full cell.

c. Optical studies: The fluorescent emis-

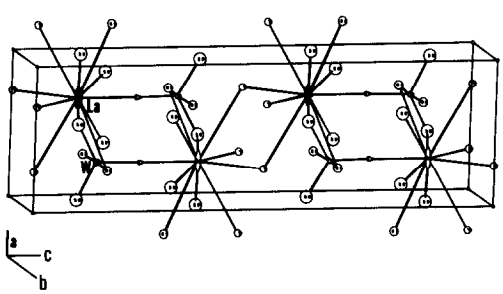

FIG. 2. Basic linkage of the $LaWO_4Cl$ structure.

TABLE V

LATTICE CONSTANTS OF THE ORTHORHOMBIC *Pbcm*-TYPE $LnBO_4X$ COMPOUNDS

Ln	*B*	*X*	*a* (Å)	*b* (Å)	*c* (Å)	*V* (Å^3)
La	W	Cl	5.898	7.863	19.286	894.41
La	W	Br	5.916	7.559	20.064	897.24
La	Mo	Cl	5.839	8.101	18.772	887.95
La	Mo	Br	5.820	7.724	19.622	882.08
Ce	W	Cl	5.890	7.798	19.217	882.64
Pr	W	Cl	5.889	7.748	19.150	873.78
Nd	W	Cl	5.879	7.691	19.108	863.97
Sm	W	Cl	5.870	7.621	10.981	849.12

sion spectra were obtained with a Perkin–Elmer MPF spectrophotometer. Diffuse reflectance data were obtained with a CARY 17 spectrophotometer. The Raman spectrum was recorded with a J–Y Laser Raman Microprobe. The spectral slit width was 3–4 cm^{-1}, and the 5145-Å line from an argon ion laser was used. The detector was an RCA C31034 phototube operated in the photon counting mode.

Results and Discussion

A. Structural Detail

The indexed powder pattern for $LaWO_4Cl$ is reported in Table III. For this data set the refined cell dimensions are a = 5.8986(5), b = 7.8620(7), and c = 19.287(1) Å; the cell volume, 894.5(1) Å^3; the calculated X-ray density, 6.26 g · ml^{-1}; and the figures of merit (*5*, *6*), M_{20} = 45 and F_{20} = 68 (0.008, 34).

The structure of $LaWO_4Cl$ is very nearly double its subcell structure and can be more clearly described in terms of the subcell. Table IV contains interatomic distances and bond angles for the 5-coordinated W and 9-coordinated La atoms. Since all atoms, except O(3), lie in mirror planes with $x = \pm\frac{1}{4}$, both W and La atoms have point symmetry m. As shown in Fig. 1a, the W atoms are in a trigonal bipyramidal coordination with the W atom 0.24 Å off the basal plane. The basal triangle is perpendicular to the mirror plane. This config-

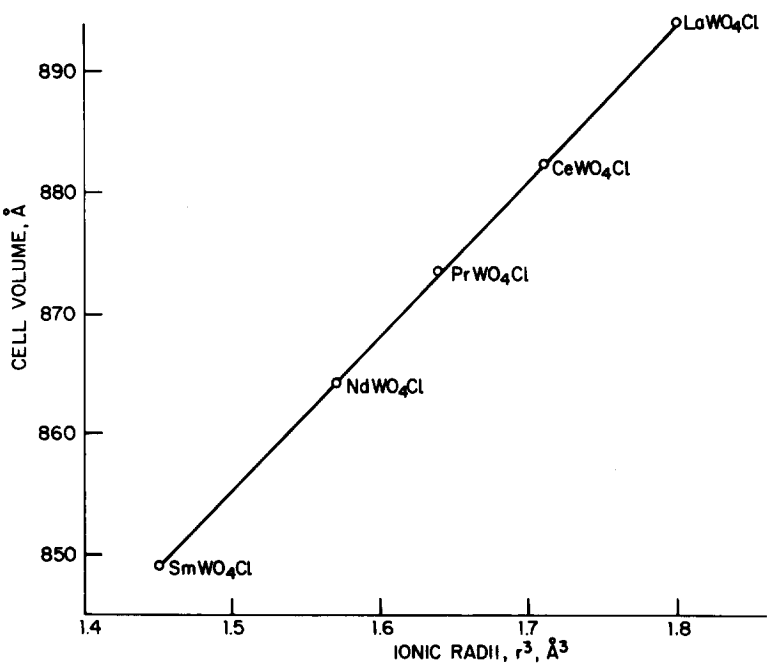

FIG. 3. Cell volumes vs r^3 for the LnWO$_4$Cl compounds.

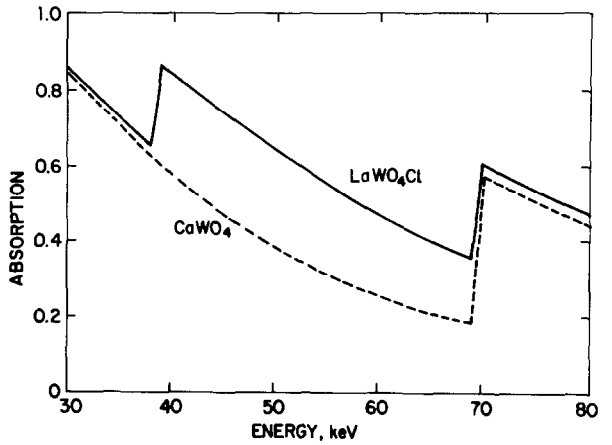

FIG. 4. X-Ray absorption for 200-μm phosphor for $LaWO_4Cl$ and $CaWO_4$.

uration can be regarded as a tetrahedron with a distortion allowing a fifth O atom to come within a bonding distance of 2.15 Å compared to an average of 1.766 Å for the other four W–O distances. W atoms are not bonded directly to any Cl atoms. The La atom in Fig. 1b is in a monocapped trigonal prismatic coordination with the axis and the capped O atom in the mirror plane. The average La–O distance is 2.489 Å; the average La–Cl distance is 2.973 Å. If the two next-nearest Cl atoms at 3.437 Å are included, then the La atom has monocapped square–antiprismatic coordination with five O atoms and four Cl atoms. La atoms are not bonded to O(2) atoms.

Figure 2 shows the basic linkage of the $LaWO_4Cl$ subcell. The basic unit consists of two W and two La atoms at the corner of a diamond with O atoms linking two neighboring metal atoms. This diamond then extends in both the *a* and *c* directions to form a layer perpendicular to the *b* axis. There are two such layers in a unit cell separated by sheets of Cl atoms.

The orthorhombic $Pbc2_1$ structure of $LaWO_4Cl$ extends to $SmWO_4Cl$. $EuWO_4Cl$ crystallizes in a new monoclinic structure

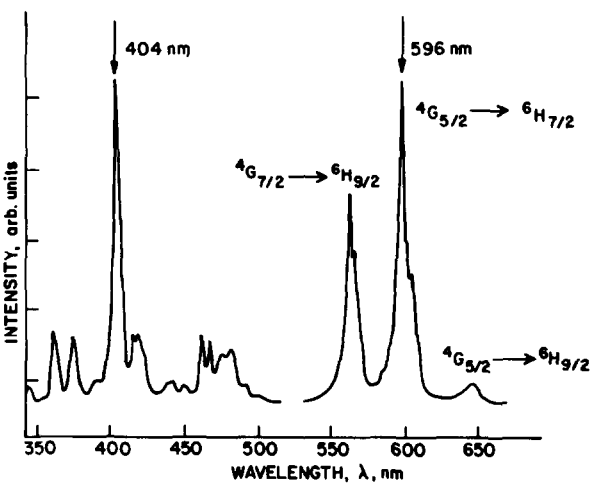

FIG. 5. Excitation and emission spectra of $La_{0.98}Sm_{0.02}WO_4Cl$.

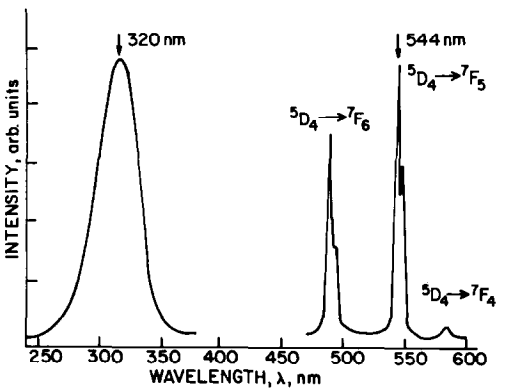

FIG. 6. Excitation and emission spectra of $La_{0.995}Tb_{0.005}WO_4Cl$.

which will be described for $GdWO_4Cl$ in a forthcoming publication. In addition to $LaWO_4Cl$, we also prepared the bromo-analog, $LaWO_4Br$, as well as the corresponding molybdates. The cell volume of both molybdates is smaller than that of the corresponding tungstate, suggesting that in this particular coordination, the Mo^{+6} ionic radius is smaller than that of W^{+6}. The cell dimensions of these compositions are summarized in Table V, and Fig. 3 shows a plot of the cell volumes as a function of the ionic radii of the rare earths.

B. Luminescence and Optical Spectra

Since $LaWO_4Cl$ represents a new structure type, it was of interest to examine it as a host for such fluorescing ions as Sm^{3+}, Eu^{3+}, and Tb^{3+}. The combination of La and W in one structure, furthermore, made it appealing as a potential X-ray phosphor, since both atoms have their $K\alpha$ absorption edges within the medically important region of 30 to 80 keV. The improved absorption over the common X-ray phosphor $CaWO_4$ is clearly evident in Fig. 4. $LaWO_4Cl$ by itself does not fluoresce at room temperature under uv or X-ray excitation. We therefore doped it with the activators Sm, Eu, and Tb. Sm^{3+} when incorporated into $LaWO_4Cl$ at the 0.01-mole level emits bright orange. Using the 404-nm excitation line, the predominant emission occurred at 596 nm, arising from the $^4G_{5/2} \rightarrow {}^6H_{7/2}$ transition. Two weaker emissions, stemming from $^4G_{7/2} \rightarrow {}^6H_{9/2}$ and $^4G_{5/2} \rightarrow {}^6H_{9/2}$ transitions, were also observed. A typical spectrum is shown in Fig. 5. Next we studied the $La_{1-x}Tb_xWO_4Cl$ system over a range of x from 0.005 to 0.05. In all cases the lower-energy emission, arising from the $^5D_4 \rightarrow {}^7F_j$ manifold, was always dominant. The spectrum of $La_{0.995}Tb_{0.005}WO_4Cl$ is shown in Fig. 6. Under 30-kVp Mo radiation X-ray excitation, this phosphor yielded a speed of 0.6 times $CaWO_4$ (Hi Plus type). The

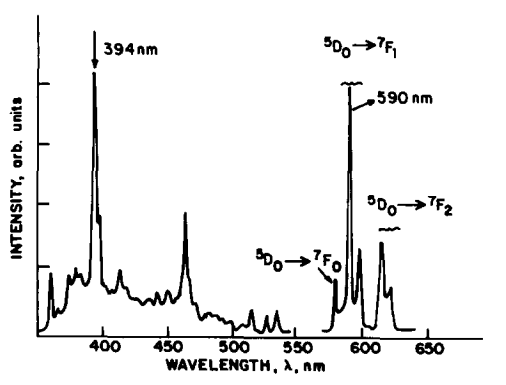

FIG. 7. Excitation and emission spectra of $La_{0.99}Eu_{0.01}WO_4Cl$.

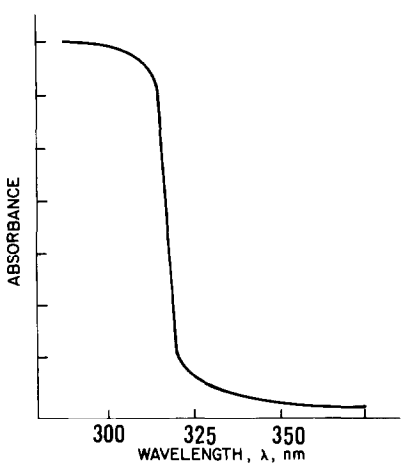

FIG. 8. Diffuse reflectance spectrum of $LaWO_4Cl$.

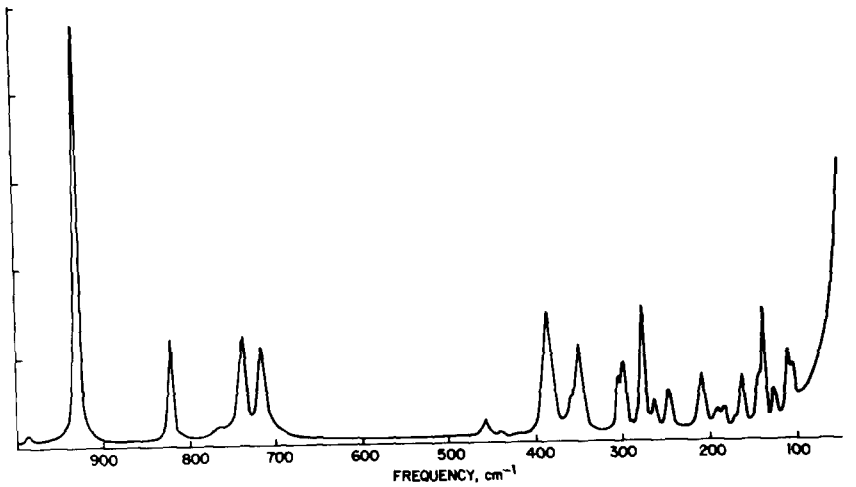

FIG. 9. Raman spectrum of $LaWO_4Cl$.

$La_{1-x}Eu_xWO_4Cl$ system was of particular interest since it constituted a case where, even at 100% occupancy of the active ion, no fluorescence quenching occurred. $EuWO_4Cl$ is a brilliantly red-emitting phosphor under uv excitation and its spectrum is shown in Fig. 7. We used the 394-nm line for excitation and the predominant emission arose from the $^5D_0 \rightarrow {}^7F_2$ transition at 616 nm. The $^5D_0 \rightarrow {}^7F_1$ and the $^5D_0 \rightarrow {}^7F_0$ transitions were also observed. Figure 8 shows the diffuse reflectance spectrum and Fig. 9 the Raman spectrum of $LaWO_4Cl$. Although we indicated earlier that the local site symmetry for W is m, it is approaching a C_{2v} configuration. For this symmetry one would expect 12 Raman active lines ($5A_1 + A_2 + 3B_1 + 3B_2$), all of which can be seen in the spectrum, provided we assign lines below 200 cm^{-1} to lattice vibrations. This makes the $LaWO_4Cl$ spectrum more complicated than that of $CaWO_4$ with T_d symmetry or Ba_2CaWO_6 with O_h symmetry. Even $La_3WO_6Cl_3$ (*7*), where W^{6+} is in trigonally prismatic D_{3h} 6-coordination, exhibits only seven Raman active lines.

In summary, we can state that $LaWO_4Cl$ constitutes a new structure type, yielding interesting fluorescence when doped with the rare earth activators Sm, Eu, and Tb. Despite improved X-ray absorption over $CaWO_4$, none of the present phosphors approach the speed of that phosphor.

Acknowledgments

The authors would like to thank Dr. B. Chase and Mrs. E. Matthews for collecting the optical data, Mr. G. Hyatt for assisting in the X-ray work and Mr. J. W. Rooney for technical assistance in materials preparation.

References

1. L. YU. KHARCHENKO, P. W. KLEVSTOV, AND L. P. SOLOVLEVA, *Sov. Phys. Dokl.* **12**, 919 (1968).
2. B. A. FRENZ, "Computing Crystallography" (H. Schenk, R. Olthof-Hazehamp, H. von Koningsveld, and G. C. Bassi, Eds.), pp. 64–71, Delft Univ. Press, Delft, Holland (1978).
3. "International Tables for X-Ray Crystallography," Vol. IV, Table 2.2B, p. 99, Kynock Press, Birmingham, England (1974).
4. *Ibid.*, Table 2.3.1, p. 148.
5. P. M. DE WOLFF, *J. Appl. Crystallogr.* **1**, 108 (1968).
6. G. S. SMITH AND R. L. SNYDER, *J. Appl. Crystallogr.* **12**, 60 (1979).
7. L. H. BRIXNER, H.-Y. CHEN, AND C. M. FORIS, *J. Solid State Chem.* **44**, 99 (1982).